J. Fluid Mech. (1971), *vol.* 45, *part* 2, *pp.* 261–279
Printed in Great Britain

Heat transfer in a cylindrical cavity

By J. L. DUDA AND J. S. VRENTAS
Process Fundamentals Research Laboratory, The Dow Chemical Company, Midland, Michigan

(Received 3 March 1970)

An analytical solution is developed to describe the unsteady-state heat transfer to a cylindrical cavity with circulating flow induced by a moving wall. The previously derived velocity field at low Reynolds numbers is incorporated into the energy equation, and the case of heat transfer to a fluid segmented by highly conducting plugs flowing in a tube with constant wall temperature is considered. Calculations of temperature distributions, average temperatures, and heat transfer coefficients as functions of time and Péclet number are presented for a specific cavity geometry, and the degree of enhancement in heat transfer caused by the recirculating flow is determined.

The methods developed in this study may be useful in obtaining analytical solutions to a variety of closed-streamline heat and mass transfer problems with known velocity fields.

Introduction

The characterization of heat or mass transfer in closed-streamline flow fields has been the object of numerous experimental and theoretical investigations. For example, Burggraf (1966) has numerically computed solutions for heat transfer in a square cavity in which flow is generated by the movement of one of the cavity walls. These finite-difference solutions were obtained for two cases under steady-state conditions for a Prandtl number of one and Reynolds numbers ranging from 0 to 400. In one case, Burggraf considered the heat transfer from a hot moving wall to cooler stationary walls, and in a second case the fixed walls were considered adiabatic and the heat generated by viscous dissipation was removed through the moving wall. The related problem of steady-state mass transport from the walls of a rectangular cavity to a fluid flowing over the cavity has been experimentally investigated by Jarrett & Sweeney (1967) who measured mass transfer rates from various locations on the walls using an evaporative surface technique.

Natural convection phenomena in rectangular cavities are good examples of heat transfer in closed-streamline flow fields involving intimate coupling between the equations of motion and the energy equation. An analytical solution describing steady-state heat transfer by laminar free convection in enclosed plane gas layers for moderately low Rayleigh numbers has been derived by Poots (1958). Gill (1966) has developed an approximate steady-state solution to the

free convection problem in a rectangular cavity which is valid for the large Rayleigh number limit where the boundary-layer equations can be utilized. Wilkes & Churchill (1966) generated finite-difference solutions of the complete set of equations describing the transient and steady-state natural convection in a rectangular enclosure.

The theory of solute extraction from falling droplets in viscous systems is of considerable practical interest. Especially important is the determination of the enhancement of the extraction rate caused by circulation currents which are set up by the viscous forces between the continuous and dispersed phases. Kronig & Brink (1950) utilized Hadamard's (1911) creeping-flow velocity field in the diffusion equation and obtained an analytical solution valid for very high Péclet numbers. For this infinite Péclet number limit, the lines of constant concentration are identical with the streamlines of the flow field. Johns & Beckmann (1966) extended this work by obtaining finite-difference solutions to the diffusion equation for this closed-streamline flow field for Péclet numbers between the stagnant-drop limit and the high circulation current limit. Finally, another example of the characterization of the heat transfer behaviour of a closed-streamline flow is the analytical solution derived by Ho, Nardacci & Nissan (1964) for a Taylor vortex system. The solution derived by these authors is valid for a small range of Taylor numbers above the critical and for a Prandtl number close to unity.

In this paper we study the heat transfer behaviour of a bolus flow velocity field of the type considered in Duda & Vrentas (1970, hereafter referred to as I) where plugs or bubbles separate elements of fluid and set up circulation patterns. The elucidation of the heat transfer mechanism for this flow is of interest because of the relatively important nature of this flow field. In addition, the techniques developed here may be useful in obtaining analytical solutions to a variety of closed-streamline heat or mass transfer problems with known velocity fields. In I, expressions were derived for the velocity fields of the two limiting cases of bolus flow, solid plugs with a no-slip boundary condition and gas bubbles with a no-drag boundary condition. Although investigation of the heat transfer characteristics is effectively equivalent for the two cases, we shall concentrate solely on the former and thus determine the temperature field in a cylindrical cavity with solid plane surfaces and a uniformly translating curved surface. This case appears to be a good approximation to the flow of blood in capillaries and also is closely related to the important problem of heat transfer in rectangular cavities. Several investigators (Prothero & Burton 1961; Oliver & Wright 1964; Oliver & Young Hoon 1968) have experimentally studied heat transfer to the bolus flow field produced by slugs of gas moving down a pipe. This case is probably best approximated by an adiabatic slug wall with a no drag boundary condition for the equations of motion. However, a theoretical treatment of the type used here is most likely somewhat inadequate since gas bubbles tend to deform, are displaced towards the top of the tube, and do not completely isolate the segments of liquid.

The analytical solution for the velocity field for the cylindrical cavity with solid walls is incorporated into the energy equation, and an analytical solution which describes unsteady-state heat transfer to the fluid in the cavity is developed.

Due to the limitation on the analytical expression for the stream function, the heat transfer analysis is valid only for low Reynolds number flows. In addition, the physical properties of the fluid are considered independent of temperature so that the energy equation and the equations of motion are not coupled. In the specific case considered in this study, heat is transferred between constant temperature cavity walls and a fluid which initially is at a uniform but different temperature. For bolus flow in a tube, this condition corresponds to the situation where the plugs which isolate the segments of fluid are at the same temperature as the tube wall; such a boundary condition would be appropriate for highly conducting solid plugs. The boundary condition on a plug surface will of course depend on the nature of the plugs which induce the recirculating flow. Although only one set of boundary conditions is treated below, the mathematical techniques presented are not limited to this specific case, and, with some modifications, a wide variety of boundary conditions could be examined.

The analytical solution developed here is used to determine average and instantaneous heat transfer coefficients as functions of time and Péclet number for a specific cavity geometry. Comparison of these results with the case of pure conduction indicates the enhancement in heat transfer due to the induced closed-streamline flow.

Solution of energy equation

We consider the laminar flow heat transfer to a Newtonian fluid in a cylindrical cavity with a uniformly translating wall. In the absence of gravitational effects the temperature and velocity fields can be assumed to be symmetrical Furthermore, the fluid motion in the cavity is assumed to be established before heating or cooling of the fluid begins. Since the properties of the fluid are considered independent of temperature, the steady velocity field calculated in I can be used and the energy equation is effectively linearized. Finally, viscous dissipation effects are considered negligible. For these conditions, the temperature field in the cavity is described by the following set of dimensionless equations:

$$\frac{\partial T}{\partial t} + V\frac{\partial T}{\partial r} + U\frac{\partial T}{\partial z} = \frac{1}{P_e}\left(\frac{\partial^2 T}{\partial r^2} + \frac{1}{r}\frac{\partial T}{\partial r} + \frac{\partial^2 T}{\partial z^2}\right), \tag{1}$$

$$T(0, r, t) = 1, \quad T(\beta, r, t) = 1, \quad T(z, 1, t) = 1, \tag{2), (3), (4)}$$

$$(\partial T/\partial r)_{r=0} = 0, \quad T(z, r, 0) = 0, \tag{5), (6)}$$

$$P_e = U_a R \hat{C}_v \rho / k, \tag{7}$$

where T is temperature, t time, r and z the radial and axial distances respectively, U and V the axial and radial velocities. P_e is the Péclet number where k is thermal conductivity, R the radius of the cavity, ρ density, U_a the velocity of the cavity wall, velocity of plugs in a pipe, and $\hat{C}_v$ the specific heat capacity at constant specific volume.

The dimensionless distance and velocity variables are as in I and the dimensionless time and temperature variables are given by the equations

$$t = t^* U_a / R, \quad T = T^* - T_0 / T_w - T_0, \tag{8), (9}$$

where T_0 is the initial temperature of the fluid and T_w is temperature of the cavity walls.

Since the components of the velocity vector for this flow field are functions of position in the cavity, it is clear that we are confronted with the problem of solving a particularly difficult parabolic partial differential equation with variable coefficients. Problems involving the simultaneous conduction and convection of heat as described by equations of the form of (1) have generally defied analytical solution except for certain special types of velocity fields such as plug and parabolic velocity profiles in a pipe (McAdams 1954). In addition, Ames & de la Cuesta (1963) and de la Cuesta & Ames (1963) have devised a method of solving this type of equation when the velocity vector can be expressed as the gradient of certain time-independent potentials. In this case, the energy equation is transformed into an equation of the Schroedinger type which is easier to solve. However, with a general velocity field, it is not always possible to obtain a separable solution to the convective heat equation; indeed, it was found that the present problem could not be solved by a standard separation of variables approach.

Analytical solutions to partial differential equations with variable coefficients can often be obtained by a formal Fourier series technique which leads to infinite systems of algebraic equations for the eigenvalues and for the coefficients of the eigenfunction expansion. As in I, a solution will be considered analytical if it can be represented by a convergent series whose terms are explicit functions of the independent variables. The Fourier series method was first used in the theory of the moon's motion by G. W. Hill in solving the ordinary differential equation which has become known as Hill's equation (Whittaker & Watson 1927; Jeffreys & Jeffreys 1956). Dennis & Poots (1956), Singh (1958), and Dennis, Mercer & Poots (1959) have since utilized the method with success in solving the partial differential equations describing various aspects of forced convection heat transfer for parallel plates, pipes, and rectangular ducts. In this study, we apply such a formal Fourier series method to the equations describing heat transfer to a cylindrical cavity and formulate the equations and methods for obtaining a sufficient number of the eigenvalues and eigenfunction coefficients to permit accurate results to be calculated.

We proceed by assuming a solution to (1)–(6) of the form

$$T(z, r, t) = 1 + \sum_{m=1}^{\infty} \sum_{n=1}^{\infty} \bar{T}_{mn}(t) \sin(n\pi z/\beta) J_0(\phi_m r), \tag{10}$$

where the ϕ_m are the zeros of

$$J_0(\phi_m) = 0. \tag{11}$$

The conditions on the boundaries of the cylindrical domain are satisfied identically by (10) and so is the initial condition if we require that

$$\bar{T}_{mn}(0) = -\frac{4[1-(-1)^n]}{n\pi\phi_m J_1(\phi_m)}. \tag{12}$$

Consequently, it remains to choose the eigenvalues and coefficients of the eigenfunction expansion so that (10) satisfies the convective heat equation, (1). Substitution of (10) into (1) and utilization of double series expansions for the convective terms in the energy equation lead to a doubly infinite set of equations for the $\overline{T}_{mn}(t)$:

$$\frac{d\overline{T}_{mn}}{dt} + \sum_{a=1}^{\infty}\sum_{b=1}^{\infty} Y_{bamn}\overline{T}_{ba} + \left[\frac{\phi_m^2 + (n\pi/\beta)^2}{P_e}\right]\overline{T}_{mn} = 0, \tag{13}$$

$$Y_{bamn} = -\frac{4\int_0^1\int_0^\beta V(r,z)\sin(a\pi z/\beta)\sin(n\pi z/\beta)r\phi_b J_1(\phi_b r)J_0(\phi_m r)\,dz\,dr}{\beta J_1^2(\phi_m)} + \frac{4\int_0^1\int_0^\beta U(r,z)a\pi\cos(a\pi z/\beta)\sin(n\pi z/\beta)rJ_0(\phi_b r)J_0(\phi_m r)\,dz\,dr}{\beta^2 J_1^2(\phi_m)}. \tag{14}$$

The doubly infinite system of linear, first-order differential equations represented by (13) is satisfied by solutions of the form

$$\overline{T}_{mn} = L_{mn}\exp[-\lambda^2 t/P_e] \tag{15}$$

if

$$L_{mn}\left[\frac{\phi_m^2 + (n\pi/\beta)^2 - \lambda^2}{P_e}\right] + \sum_{a=1}^{\infty}\sum_{b=1}^{\infty} Y_{bamn}L_{ba} = 0 \tag{16}$$

for all mn. Equation (16) represents a doubly infinite set of linear, algebraic, homogeneous equations for the L_{mn}. The eigenvalues, λ^2, are determined from the condition for non-vanishing L_{mn}, namely that the determinant of the coefficients in the system of equations represented by (16) must vanish. The doubly infinite set of eigenvalues can, in principle, then be obtained from the algebraic equation resulting from setting this determinant equal to zero. Rather than deal with infinite determinants, we utilize the infinite system, (16), directly to evaluate the pqth eigenvalue, λ_{pq}^2, and its associated eigenvector, L_{mn}^{pq}. Consequently, if the eigenvector is normalized using

$$K_{mn}^{pq} = \frac{L_{mn}^{pq}}{L_{pq}^{pq}}, \tag{17}$$

then each eigenvalue and its normalized eigenvector can be determined directly from the following doubly infinite system of equations:

$$\frac{\phi_p^2 + (q\pi/\beta)^2 - \lambda_{pq}^2}{P_e} + \sum_{a=1}^{\infty}\sum_{b=1}^{\infty} Y_{bapq}K_{ba}^{pq} = 0, \tag{18}$$

$$K_{mn}^{pq}\left[\frac{\phi_m^2 + (n\pi/\beta)^2 - \lambda_{pq}^2}{P_e}\right] + \sum_{a=1}^{\infty}\sum_{b=1}^{\infty} Y_{bamn}K_{ba}^{pq} = 0, \quad mn \neq pq. \tag{19}$$

If it is assumed that the eigenvalues are distinct, then the solution of (13) takes the form

$$\overline{T}_{mn}(t) = \sum_{p=1}^{\infty}\sum_{q=1}^{\infty} M_{pq}K_{mn}^{pq}\exp[-\lambda_{pq}^2 t/P_e], \tag{20}$$

where we have set

$$L_{pq}^{pq} = M_{pq}. \tag{21}$$

In addition, the initial condition for the $\bar{T}_{mn}$, (12), is satisfied if the M_{pq} are calculated from the following doubly infinite set of equations:

$$-\frac{4[1-(-1)^n]}{n\pi\,\phi_m J_1(\phi_m)} = \sum_{p=1}^{\infty}\sum_{q=1}^{\infty} M_{pq} K_{mn}^{pq}. \tag{22}$$

Finally, it follows from (10) and (20) that the solution to (1)–(6) can be expressed as

$$T = 1 + \sum_{m=1}^{\infty}\sum_{n=1}^{\infty}\sum_{p=1}^{\infty}\sum_{q=1}^{\infty} M_{pq} K_{mn}^{pq} \sin(n\pi z/\beta) J_0(\phi_m r) \exp[-\lambda_{pq}^2 t/P_e]. \tag{23}$$

Calculation of eigenvalues, eigenvectors, and eigenfunction coefficients

In this section, the formalism for the calculation of the eigenvalues, λ_{pq}^2, the associated eigenvectors, K_{mn}^{pq}, and the eigenfunction coefficients, M_{pq}, is presented. To facilitate this development we first briefly sketch the method used for calculating the four-suffix coefficients, Y_{bamn}, and, in addition, discuss the eigenvalue problem for vector spaces with an infinite number of dimensions.

Calculation of Y_{bamn}

Introduction of the definition of the stream function into (14) and appropriate integration by parts yield the following expression for the Y_{bamn}:

$$Y_{bamn} = \frac{4\int_0^1\int_0^\beta \psi(r,z)\,\phi_b n\pi \sin(a\pi z/\beta)\cos(n\pi z/\beta) J_1(\phi_b r) J_0(\phi_m r)\,dz\,dr}{\beta^2 J_1^2(\phi_m)} - \frac{4\int_0^1\int_0^\beta \psi(r,z)\,\phi_m a\pi \sin(n\pi z/\beta)\cos(a\pi z/\beta) J_1(\phi_m r) J_0(\phi_b r)\,dz\,dr}{\beta^2 J_1^2(\phi_m)}. \tag{24}$$

The spatial dependence of the stream function was determined in I and for the present purpose it is convenient to utilize these previous results to formulate a double series representation for ψ. Substitution of this double series form into (24) reduces the problem of calculating the Y_{bamn} to evaluating a trigonometric integral and an integral involving Bessel functions. The first integral can be evaluated exactly whereas the second must be calculated by integration of an infinite series. Details of these steps are straightforward and are omitted. An aid to the computation is the fact that the Y_{bamn} exhibit the following symmetry property:

$$Y_{mnba} = -\frac{J_1^2(\phi_m) Y_{bamn}}{J_1^2(\phi_b)}. \tag{25}$$

Eigenvalue problem for an infinite-dimensional vector space

Determination of the λ^2 from (16) is, on the surface at least, just the classical eigenvalue problem, and (16) can be re-expressed as

$$\left(\mathbf{A} - \frac{\lambda^2}{P_e}\mathbf{I}\right)\mathbf{L} = \mathbf{0}, \tag{26}$$

where **I** is an infinite unit matrix, **L** is the appropriate infinite column vector, and **A** is the infinite square matrix whose non-diagonal elements are the Y_{bamn} and whose diagonal elements are given by

$$A_{mnmn} = \frac{\phi_m^2 + (n\pi/\beta)^2}{P_e}. \tag{27}$$

It is clear from (25) that **A** is not symmetric so, assuming that infinite matrices behave like finite matrices, it is not possible to deduce if the eigenvalues of **A** are real.

It does not always follow that the eigenvalue problem for infinite matrices is completely analogous to that for matrices of finite size. For example, there exist relatively simple infinite matrices that have no eigenvalues at all. Consequently, the eigenvalue problem must be reformulated if linear vector spaces with an infinite number of dimensions are to be included in the general formalism. Cooke (1953) discusses von Neumann's analysis of this problem which is of great importance in the solution of many problems of quantum physics. If the eigenvalue spectrum of an infinite matrix is such that any given vector can be represented arbitrarily closely by a linear combination of basis vectors which form a countable or denumerable set, then the eigenvalue problem is essentially equivalent to that for a space of finite dimensions. Differences exist simply because infinite rather than finite matrices are involved and because attention must be given to the mathematical questions of convergence for the infinite operations required. In some instances, however, the eigenvector basis is non-denumerable, consisting of a continuum of vectors; for this case, changes must be made in the eigenvalue problem. It is not probable that such difficulties will occur in the present case, and we proceed on the assumption that the eigenvalue problem for the infinite matrix **A** is essentially no different than that for a finite matrix.

Conjugate gradient method for the eigenvalues

Determination of the eigenvalues and eigenvectors of the infinite matrix **A** was accomplished by directly solving the doubly infinite set of equations given by (18) and (19) rather than by utilizing the more standard techniques usually applied to matrices of finite size. The method of reduction (Kantorovich & Krylov 1958) was used to solve the non-linear infinite system, and progressively larger finite systems were employed in order to asymptotically approach the solution to the infinite system. Perhaps the most efficient way to obtain solutions of the finite systems is by application of a successive approximation method. However, iterative methods are not convergent in this case since the non-diagonal or convective terms of the infinite **A** matrix are not small relative to the diagonal or conductive entries, except at small Péclet numbers where heat conduction is the prime mode of transport.

Consequently, it is convenient to apply a conjugate gradient method of the type outlined by Goldfarb & Lapidus (1968) to solve the non-linear system of equations. By combining (18) and (19) it is possible to put the non-linear set into

the following form:

$$F_{mn} = K_{mn}^{pq}\left[\frac{\phi_m^2+(n\pi/\beta)^2-\phi_p^2-(q\pi/\beta)^2}{P_e} - \sum_{a=1}^{\infty}\sum_{b=1}^{\infty} Y_{bapq}K_{ba}^{pq}\right] + \sum_{a=1}^{\infty}\sum_{b=1}^{\infty} Y_{bamn}K_{ba}^{pq} = 0, \quad mn \neq pq. \tag{28}$$

The problem of finding a solution of the system represented by (28) can then be reduced to the problem of determining the values of K_{mn}^{pq} for which the function

$$\mathscr{F}(K_{kl}^{pq}) = \sum_{\substack{m=1 \\ mn\neq pq}}^{\infty}\sum_{n=1}^{\infty} F_{mn}^2(K_{kl}^{pq}) \tag{29}$$

assumes a minimum value (equal to zero). Once the K_{mn}^{pq}, the components of the normalized eigenvector, are calculated using the conjugate gradient approach, the associated eigenvalue, λ_{pq}^2, is determined directly from (18). The quadratic convergence property of the conjugate gradient method was essential in obtaining converged eigenvectors in a reasonable amount of computer time since application of the well-known steepest descent technique to this problem led to extremely slow rates of convergence.

Since it is of course not possible to obtain all of the eigenvalues of the matrix, we are interested in determining only the first few smallest ones since these will suffice for most heat transfer calculations. By the method proposed above, it is possible by poor choice of the starting vector to obtain the eigenvector for one of the larger eigenvalues. This difficulty is avoided in the following manner. As is shown below, all the eigenvalues and associated eigenvectors are known for $P_e = 0$. Hence, it is possible to start the calculation using the eigenvector at $P_e = 0$ and calculate this vector as a function of Péclet number by gradually increasing the Péclet number. Thus, a good estimate of the starting vector is always available, and it is possible to calculate the local minimum appropriate to the eigenvalue of interest without much difficulty.

Variational method for calculation of the M_{mn}

The M_{mn}, the coefficients of the eigenfunction expansion, can be determined by directly solving the doubly infinite set of equations represented by (22) by using the method of reduction in conjunction with the conjugate gradient technique. However, more accurate results can be obtained with equivalent finite system approximations to the infinite system if a variational method is applied in the manner suggested by Dennis & Poots (1956) and by Singh (1958). The result of this minimization can ultimately be expressed as

$$-4\sum_{m=1}^{\infty}\sum_{n=1}^{\infty}\frac{K_{mn}^{ba}[1-(-1)^n]J_1(\phi_m)}{n\pi\phi_m} = \sum_{m=1}^{\infty}\sum_{n=1}^{\infty}\sum_{p=1}^{\infty}\sum_{q=1}^{\infty} M_{pq}J_1^2(\phi_m)K_{mn}^{pq}K_{mn}^{ba}. \tag{30}$$

The solution of the doubly infinite linear system represented by (30) can be derived by utilization of the method of reduction and the conjugate gradient technique.

Heat transfer coefficients

The heat transfer capabilities of the recirculating flow field in the cylindrical cavity are perhaps better assessed by examination of average temperatures and heat transfer coefficients rather than spatial temperature distributions. Consequently, in this section we derive the necessary formulas for the calculation of the time variations of the average temperature in the cavity, the instantaneous heat transfer coefficient, and the average heat transfer coefficient. Utilization of (23) and integration over the volume of the cavity produce the expression for the time dependence of the average temperature,

$$T_a(t) = 1 + \sum_{m=1}^{\infty}\sum_{n=1}^{\infty}\sum_{p=1}^{\infty}\sum_{q=1}^{\infty}\frac{2W_{pqmn}\exp\left[-\lambda_{pq}^2 t/P_e\right]}{\phi_m n\pi}, \tag{31}$$

$$W_{pqmn} = M_{pq}K_{mn}^{pq}J_1(\phi_m)\left[1-(-1)^n\right]. \tag{32}$$

An instantaneous heat transfer coefficient, h_i, can be defined by the equation

$$q_i = 2h_i\pi R(L+R)(T_w - T_a^*), \tag{33}$$

where q_i is the instantaneous heat flow into the cavity and T_a^* is the dimensional average temperature. Hence, from (23), (31), and (33) it can be shown that the instantaneous Nusselt number is given by the following result:

$$\frac{h_i R}{k} = \frac{\sum_{m=1}^{\infty}\sum_{n=1}^{\infty}\sum_{p=1}^{\infty}\sum_{q=1}^{\infty}W_{pqmn}\left[\frac{\phi_m\beta}{n\pi}+\frac{n\pi}{\beta\phi_m}\right]\exp\left[-\frac{\lambda_{pq}^2 t}{P_e}\right]}{(1+\beta)\sum_{m=1}^{\infty}\sum_{n=1}^{\infty}\sum_{p=1}^{\infty}\sum_{q=1}^{\infty}\frac{2W_{pqmn}\exp\left[-\lambda_{pq}^2 t/P_e\right]}{\phi_m n\pi}}. \tag{34}$$

Similarly, an average heat transfer coefficient, h_a, can be defined by the equation

$$Q/t^* = 2h_a\pi R(R+L)\tfrac{1}{2}[(T_w - T_0)+(T_w - T_a^*)], \tag{35}$$

where t^* is the dimensional time and Q is the total heat added to the fluid in the cavity from $t^* = 0$ to $t^* = t^*$. It can be shown that (35) yields the following expression for the average Nusselt number:

$$h_a R/k = P_e\beta T_a/(1+\beta)t(2-T_a). \tag{36}$$

It is of interest to see how the results of this study simplify for the case where the wall of the cavity is not translating so that the fluid is quiescent and heat is transferred solely by conduction. For this situation, it is clear that

$$\psi = 0, \quad Y_{bamn} = 0. \tag{37}$$

Hence, it follows from (18) and (19) that

$$\lambda_{pq}^2 = \phi_p^2 + (q\pi/\beta)^2, \tag{38}$$

$$K_{mn}^{pq} = 0, \quad mn \neq pq \tag{39}$$

and, thus, (22) simplifies to

$$M_{mn} = -\frac{4[1-(-1)^n]}{n\pi\phi_m J_1(\phi_m)}. \tag{40}$$

Finally, (23) can be reduced to

$$T(z,r,t) = 1 + \sum_{m=1}^{\infty}\sum_{n=1}^{\infty} M_{mn} \sin(n\pi z/\beta) J_0(\phi_m r) \exp\left[-\frac{\phi_m^2 + (n\pi/\beta)^2}{P_e} t\right], \quad (41)$$

which is of course the equation that has been derived for heat conduction in a cylinder by a standard separation of variables approach (Carslaw & Jaeger 1959). It can also be easily shown that, for a quiescent cavity, (31) and (34) take the following forms:

$$T_a(t) = 1 - \sum_{m=1}^{\infty}\sum_{n=1}^{\infty} \frac{8[1-(-1)^n]^2}{\phi_m^2 n^2 \pi^2} \exp\left[-\frac{\phi_m^2 + (n\pi/\beta)^2}{P_e} t\right], \quad (42)$$

$$\frac{h_i R}{k} = \frac{\sum_{m=1}^{\infty}\sum_{n=1}^{\infty} \frac{[1-(-1)^n]^2}{\phi_m n\pi}\left[\frac{\phi_m \beta}{n\pi} + \frac{n\pi}{\phi_m \beta}\right] \exp\left[-\frac{\phi_m^2 + (n\pi/\beta)^2}{P_e} t\right]}{2(1+\beta)\sum_{m=1}^{\infty}\sum_{n=1}^{\infty} \frac{[1-(-1)^n]^2}{\phi_m^2 n^2 \pi^2} \exp\left[-\frac{\phi_m^2 + (n\pi/\beta)^2}{P_e} t\right]}. \quad (43)$$

A cavity with stagnant fluid is representative of the idealized case where a train of plugs moves down a pipe segmented by fluid which is in plug flow.

If we now go back to the equations valid for a cavity with a recirculating flow field, it is clear that these equations also yield (38)–(43) in the limit as $P_e \to 0$. This is of course to be expected since, as the Péclet number becomes very small, the heat transfer by convection becomes insignificant when compared to heat transfer by conduction. Hence, for very low Péclet numbers the heat transport characteristics of a cavity with a recirculating fluid become effectively indistinguishable from those of a cavity with a stagnant fluid.

Finally, the long-time asymptote of the instantaneous Nusselt number for the recirculating flow field is given by

$$\frac{h_i R}{k}(\infty) = \frac{\sum_{m=1}^{\infty}\sum_{n=1}^{\infty} K_{mn}^{11} J_1(\phi_m)\left[\frac{\phi_m \beta}{n\pi} + \frac{n\pi}{\beta \phi_m}\right][1-(-1)^n]}{(1+\beta)\sum_{m=1}^{\infty}\sum_{n=1}^{\infty} \frac{2K_{mn}^{11} J_1(\phi_m)[1-(-1)^n]}{\phi_m n\pi}}, \quad (44)$$

whereas for a stagnant flow field (or for a recirculating flow field at low Péclet numbers) this quantity takes the following form

$$\frac{h_i R}{k}(\infty) = \frac{\phi_1^2 \beta^2 + \pi^2}{2\beta(1+\beta)}. \quad (45)$$

It should also be noted that the average Nusselt number in a cavity at any given time can never exceed the value given by the expression:

$$\left(\frac{h_a R}{k}\right)_{\max} = \frac{P_e \beta}{(1+\beta)t}. \quad (46)$$

Results and discussion

Detailed calculations were carried out for a cylindrical cavity with an aspect ratio of $\beta = 1$ for Péclet numbers ranging from 0 to 200. In principle, it is possible to determine the heat transfer characteristics of a cavity for any Péclet number and for any aspect ratio from the above equations. In practice, however, although there is no difficulty in covering a wide range of Péclet numbers, the computations become somewhat cumbersome for large values of β. This difficulty results because the eigenvalues lie closer together as β is increased. Although results could be obtained without excessive difficulty for aspect ratios as high as $\beta = 5$, in this study we concentrate on conducting a thorough investigation of the heat transfer behaviour for a single cavity geometry. In addition, no calculations were made for Péclet numbers higher than 200 since the transition from the effectively stagnant flow régime to the large circulation current régime is essentially complete at this value of Péclet number.

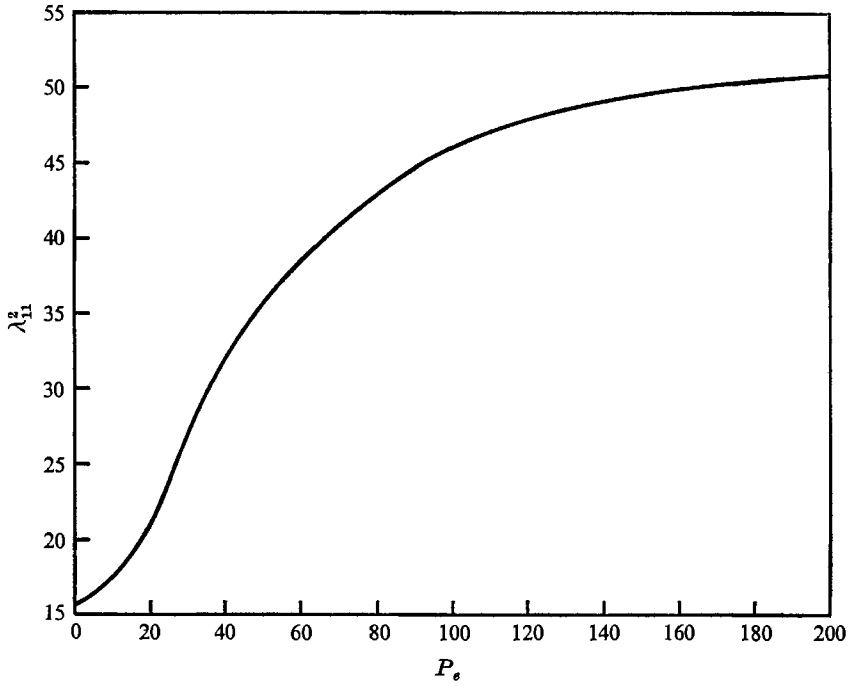

FIGURE 1. Dependence of λ_{11}^2 on Péclet number.

Eigenvectors and the associated eigenvalues were computed for $\beta = 1$ by using the conjugate gradient method to solve 35 or 99 non-linear equations of the type represented by (28). Increase of the size of the finite system approximation to the infinite system yielded insignificant changes for the first 25 components (for K_{mn}^{pq}, $m = 1$ to 5, $n = 1$ to 5) of the eigenvectors for at least the four smallest eigenvalues. The first 36 components of the eigenvector for the smallest eigenvalue, λ_{11}^2, are shown in table 1 for five values of the Péclet number. In

		Péclet number				
m	n	10	25	45	75	100
1	1	1·000	1·000	1·000	1·000	1·000
1	2	$-2{\cdot}156\times10^{-1}$	$-4{\cdot}657\times10^{-1}$	$-5{\cdot}464\times10^{-1}$	$-4{\cdot}514\times10^{-1}$	$-3{\cdot}723\times10^{-1}$
1	3	$2{\cdot}789\times10^{-2}$	$1{\cdot}391\times10^{-1}$	$2{\cdot}300\times10^{-1}$	$1{\cdot}924\times10^{-1}$	$1{\cdot}338\times10^{-1}$
1	4	$1{\cdot}879\times10^{-3}$	$-2{\cdot}549\times10^{-2}$	$-8{\cdot}720\times10^{-2}$	$-1{\cdot}161\times10^{-1}$	$-1{\cdot}116\times10^{-1}$
1	5	$-8{\cdot}896\times10^{-4}$	$1{\cdot}672\times10^{-3}$	$2{\cdot}350\times10^{-2}$	$4{\cdot}404\times10^{-2}$	$4{\cdot}269\times10^{-2}$
1	6	$1{\cdot}222\times10^{-3}$	$3{\cdot}283\times10^{-3}$	$-4{\cdot}342\times10^{-4}$	$-1{\cdot}456\times10^{-2}$	$-2{\cdot}306\times10^{-2}$
2	1	$-3{\cdot}839\times10^{-2}$	$-2{\cdot}321\times10^{-1}$	$-5{\cdot}863\times10^{-1}$	$-9{\cdot}573\times10^{-1}$	$-1{\cdot}167$
2	2	$7{\cdot}643\times10^{-2}$	$1{\cdot}987\times10^{-1}$	$3{\cdot}203\times10^{-1}$	$3{\cdot}532\times10^{-1}$	$3{\cdot}362\times10^{-1}$
2	3	$-1{\cdot}220\times10^{-2}$	$-5{\cdot}947\times10^{-2}$	$-9{\cdot}194\times10^{-2}$	$-5{\cdot}363\times10^{-2}$	$-9{\cdot}061\times10^{-3}$
2	4	$6{\cdot}316\times10^{-3}$	$3{\cdot}088\times10^{-2}$	$7{\cdot}295\times10^{-2}$	$1{\cdot}007\times10^{-1}$	$1{\cdot}069\times10^{-1}$
2	5	$-1{\cdot}103\times10^{-3}$	$-9{\cdot}896\times10^{-3}$	$-2{\cdot}978\times10^{-2}$	$-3{\cdot}666\times10^{-2}$	$-2{\cdot}760\times10^{-2}$
2	6	$-2{\cdot}110\times10^{-4}$	$2{\cdot}084\times10^{-3}$	$1{\cdot}277\times10^{-2}$	$2{\cdot}750\times10^{-2}$	$3{\cdot}366\times10^{-2}$
3	1	$3{\cdot}408\times10^{-2}$	$1{\cdot}998\times10^{-1}$	$4{\cdot}889\times10^{-1}$	$7{\cdot}786\times10^{-1}$	$9{\cdot}327\times10^{-1}$
3	2	$-3{\cdot}316\times10^{-3}$	$-6{\cdot}790\times10^{-2}$	$-2{\cdot}070\times10^{-1}$	$-2{\cdot}756\times10^{-1}$	$-2{\cdot}684\times10^{-1}$
3	3	$-6{\cdot}621\times10^{-4}$	$5{\cdot}269\times10^{-3}$	$3{\cdot}133\times10^{-2}$	$3{\cdot}806\times10^{-2}$	$2{\cdot}555\times10^{-2}$
3	4	$-6{\cdot}876\times10^{-3}$	$-1{\cdot}745\times10^{-2}$	$-4{\cdot}180\times10^{-2}$	$-8{\cdot}007\times10^{-2}$	$-9{\cdot}874\times10^{-2}$
3	5	$1{\cdot}764\times10^{-3}$	$8{\cdot}851\times10^{-3}$	$1{\cdot}681\times10^{-2}$	$1{\cdot}716\times10^{-2}$	$1{\cdot}066\times10^{-2}$
3	6	$-1{\cdot}081\times10^{-3}$	$-5{\cdot}400\times10^{-3}$	$-1{\cdot}345\times10^{-2}$	$-2{\cdot}015\times10^{-2}$	$-2{\cdot}428\times10^{-2}$
4	1	$-1{\cdot}135\times10^{-2}$	$-8{\cdot}288\times10^{-2}$	$-2{\cdot}598\times10^{-1}$	$-4{\cdot}701\times10^{-1}$	$-5{\cdot}776\times10^{-1}$
4	2	$-4{\cdot}373\times10^{-3}$	$2{\cdot}498\times10^{-2}$	$1{\cdot}132\times10^{-1}$	$1{\cdot}750\times10^{-1}$	$1{\cdot}784\times10^{-1}$
4	3	$1{\cdot}539\times10^{-3}$	$4{\cdot}014\times10^{-4}$	$-2{\cdot}426\times10^{-2}$	$-5{\cdot}568\times10^{-2}$	$-6{\cdot}866\times10^{-2}$
4	4	$3{\cdot}711\times10^{-3}$	$1{\cdot}036\times10^{-2}$	$3{\cdot}209\times10^{-2}$	$7{\cdot}056\times10^{-2}$	$9{\cdot}177\times10^{-2}$
4	5	$-1{\cdot}161\times10^{-3}$	$-5{\cdot}681\times10^{-3}$	$-1{\cdot}142\times10^{-2}$	$-1{\cdot}215\times10^{-2}$	$-6{\cdot}921\times10^{-3}$
4	6	$1{\cdot}257\times10^{-3}$	$4{\cdot}743\times10^{-3}$	$1{\cdot}017\times10^{-2}$	$1{\cdot}574\times10^{-2}$	$2{\cdot}033\times10^{-2}$
5	1	$3{\cdot}152\times10^{-3}$	$3{\cdot}243\times10^{-2}$	$1{\cdot}303\times10^{-1}$	$2{\cdot}591\times10^{-1}$	$3{\cdot}159\times10^{-1}$
5	2	$4{\cdot}250\times10^{-3}$	$-3{\cdot}158\times10^{-3}$	$-4{\cdot}844\times10^{-2}$	$-9{\cdot}798\times10^{-2}$	$-1{\cdot}031\times10^{-1}$
5	3	$-9{\cdot}924\times10^{-4}$	$-1{\cdot}290\times10^{-3}$	$1{\cdot}727\times10^{-2}$	$5{\cdot}617\times10^{-2}$	$7{\cdot}510\times10^{-2}$
5	4	$-1{\cdot}614\times10^{-3}$	$-6{\cdot}489\times10^{-3}$	$-2{\cdot}452\times10^{-2}$	$-5{\cdot}729\times10^{-2}$	$-7{\cdot}200\times10^{-2}$
5	5	$5{\cdot}648\times10^{-4}$	$3{\cdot}472\times10^{-3}$	$9{\cdot}510\times10^{-3}$	$1{\cdot}369\times10^{-2}$	$9{\cdot}993\times10^{-3}$
5	6	$-9{\cdot}820\times10^{-4}$	$-3{\cdot}482\times10^{-3}$	$-8{\cdot}349\times10^{-3}$	$-1{\cdot}685\times10^{-2}$	$-2{\cdot}432\times10^{-2}$
6	1	$-7{\cdot}243\times10^{-4}$	$-1{\cdot}145\times10^{-2}$	$-6{\cdot}108\times10^{-2}$	$-1{\cdot}490\times10^{-1}$	$-1{\cdot}978\times10^{-1}$
6	2	$-3{\cdot}098\times10^{-3}$	$-3{\cdot}905\times10^{-3}$	$2{\cdot}001\times10^{-2}$	$8{\cdot}184\times10^{-2}$	$1{\cdot}225\times10^{-1}$
6	3	$7{\cdot}402\times10^{-4}$	$2{\cdot}179\times10^{-3}$	$-1{\cdot}204\times10^{-2}$	$-6{\cdot}931\times10^{-2}$	$-1{\cdot}207\times10^{-1}$
6	4	$5{\cdot}052\times10^{-4}$	$3{\cdot}090\times10^{-3}$	$1{\cdot}646\times10^{-2}$	$5{\cdot}499\times10^{-2}$	$8{\cdot}890\times10^{-2}$
6	5	$-2{\cdot}389\times10^{-4}$	$-2{\cdot}055\times10^{-3}$	$-7{\cdot}975\times10^{-3}$	$-2{\cdot}123\times10^{-2}$	$-3{\cdot}546\times10^{-2}$
6	6	$6{\cdot}450\times10^{-4}$	$2{\cdot}413\times10^{-3}$	$6{\cdot}753\times10^{-3}$	$1{\cdot}642\times10^{-2}$	$2{\cdot}874\times10^{-2}$

TABLE 1. Calculated values of K_{mn}^{11}

	Péclet number				
	10	25	45	75	100
λ_{11}^2	17·2086	24·1244	33·9737	41·7634	45·1052
λ_{12}^3	44·0564	52·2865	76·7916	100·0058	105·4450
λ_{21}^2	43·8928	48·9918	62·5298	88·9028	93·7213
M_{11}	−2·0561	−2·0124	−1·7916	−1·6092	−1·5452
M_{12}	0·6920	−0·1769	0·0194	−0·5122	−1·3784
M_{21}	1·9794	0·6513	0·3523	−0·4594	−1·5719

TABLE 2. Calculated eigenvalues and eigenfunction coefficients

addition, the three smallest eigenvalues and the appropriate coefficients of the eigenfunction expansion are presented in table 2 for the same five Péclet numbers. These three eigenvalues and the associated eigenvectors and eigenfunction coefficients are sufficient for accurate heat transfer calculations for all but the smallest times. The dependence of λ_{11}^2 on Péclet number is portrayed in figure 1 and it is evident that this eigenvalue is very close to its infinite Péclet number asymptote at $P_e = 200$.

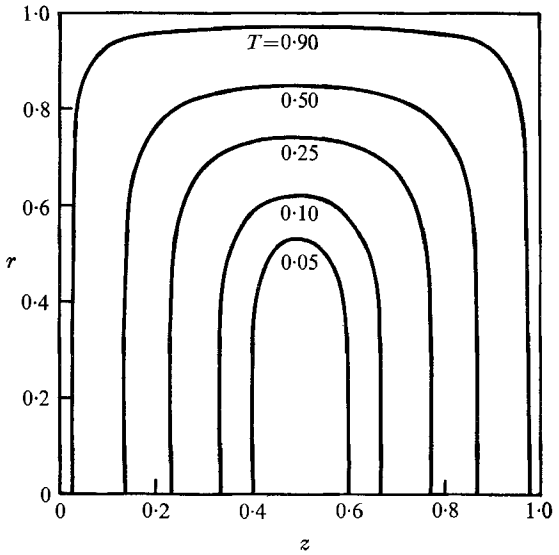

FIGURE 2. Isotherms for pure conduction heat transfer, $t/P_e = 0{\cdot}02$.

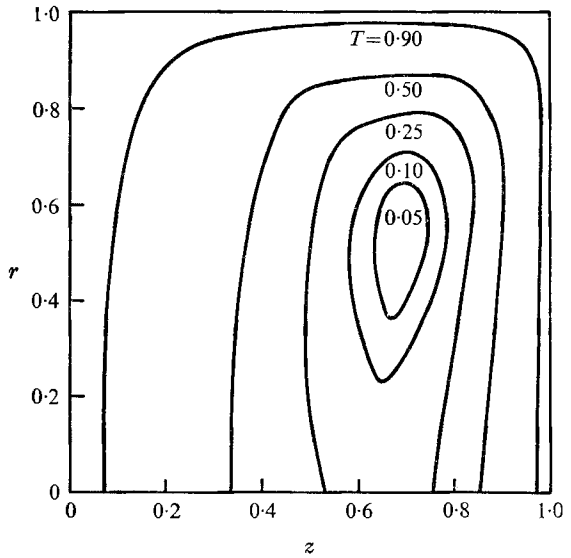

FIGURE 3. Isotherms for induced flow heat transfer, $P_e = 25$, $t/P_e = 0{\cdot}02$.

The temperature field in a cavity with no fluid circulation or with circulation in the limit of low Péclet numbers is symmetrical with the minimum temperature occurring at $z = 0{\cdot}5$ and $r = 0$. The isotherms for this case for $t/P_e = 0{\cdot}02$ are shown in figure 2. As the Péclet number increases and the convective terms in the energy equation become important, the symmetry of the temperature field is destroyed and the position of the temperature minimum moves away from the centreline. This phenomenon is evident in figure 3 where isotherms are presented for $P_e = 25$ and $t/P_e = 0{\cdot}02$. The temperature minimum is forced from left to right and away from the centreline because the counterclockwise flow carries fluid which has passed by the solid walls of the cavity which are of course at the maximum possible temperature.

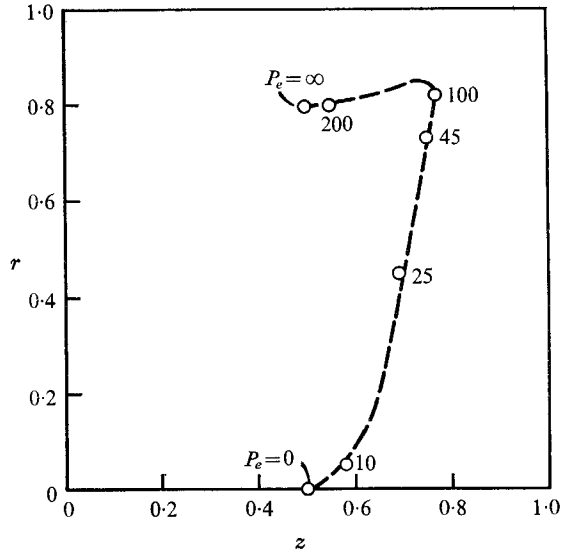

FIGURE 4. Effect of Péclet number on location of asymptotic minimum temperature.

In the classical Graetz problem for forced convection in a tube, it is well known that the local Nusselt number approaches an asymptote and that the temperature profile does not change shape as soon as the temperature boundary layers meet at the tube axis (Eckert & Drake 1959). An asymptotic instantaneous Nusselt number and an asymptotic temperature profile are also observed for the cylindrical cavity. The position of the minimum temperature for these asymptotic temperature distributions is depicted in figure 4 as a function of the Péclet number. The location of the temperature extremum progresses from the low Péclet number or conduction limit at $z = 0{\cdot}5$, $r = 0$ to the infinite Péclet number or large circulation current limit at $z = 0{\cdot}5$, $r = 0{\cdot}794$. At very high Péclet numbers, the isotherms of the temperature field are identical to the streamlines of the velocity field for all but the earliest times. Hence, the vortex centre and the temperature minimum necessarily coincide for this limiting case. The locus of the minima for intermediate Péclet numbers is similar to that observed by

Johns & Beckmann (1966) for the concentration maxima in the circulating drop problem. These authors presented a sequence of asymptotic concentration profiles which demonstrated the progression from the pure diffusion limit to the Kronig & Brink infinite Péclet number limit. In addition, in a linearized analysis of circular eddies, Burggraf (1966) showed that the location of the vortex centre follows a path strikingly similar to that of the present study as the Reynolds number is increased from zero to infinity.

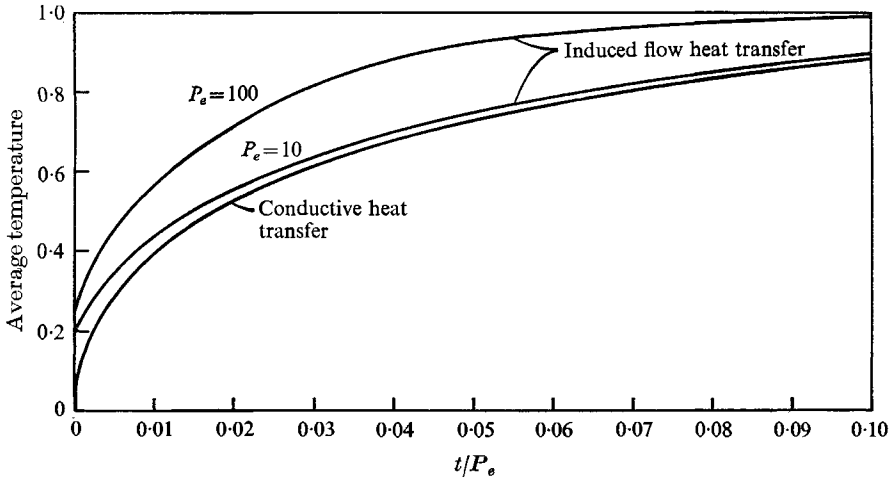

FIGURE 5. Time dependence of dimensionless average temperature.

An example of the enhanced heat transfer caused by the circulation currents is illustrated in figure 5. This graph indicates the magnitude of the more rapid ascent of the average temperature in the cavity as the Péclet number is increased from the zero Péclet number or pure conduction limit. The increased efficiency of the induced flow heat transfer of course becomes less pronounced at the longer times.

The time decay of the average Nusselt number for both actual and idealized bolus flow (uniform velocity profile in a fluid between plugs moving down a circular pipe) for $P_e = 100$ is shown in figure 6. The superiority of induced flow heat transfer is greatest at the short contact times since the average Nusselt number for both cases approaches zero at long times. The average Nusselt number for both induced flow and conductive heat transport is shown as a function of Péclet number for $t = 0{\cdot}1$ in figure 7. This graph is similar to the familiar Nusselt number–Péclet number plots for fixed length to diameter ratios which are usually presented for forced convection heat transfer in laminar tube flow (Eckert & Drake 1959). As would be expected, the effectiveness of the induced flow heat transfer over conductive heat transfer increases with increasing Péclet number. It should also be noted that, as in the pipe flow case, there exists an upper limit for the average Nusselt number given by (46). The use of a Péclet number to describe conductive heat transfer is of course somewhat artificial; however, it is convenient here to use a Péclet number based on the velocity of the plugs to compare actual and idealized bolus flow in a pipe.

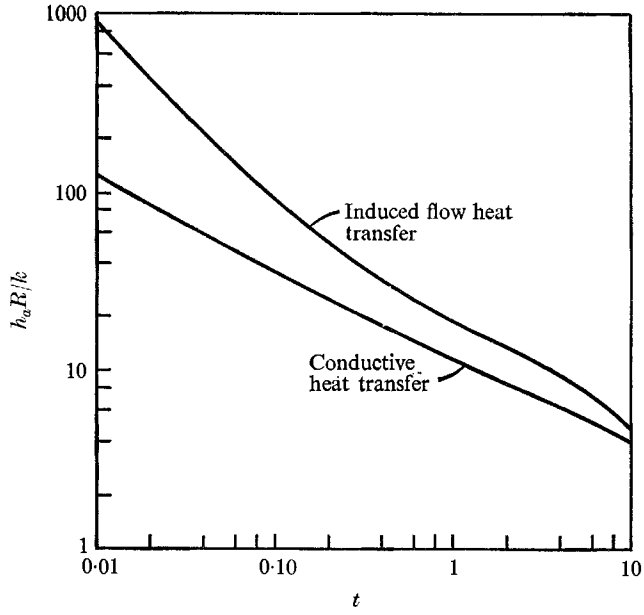

FIGURE 6. Time dependence of average Nusselt number for $P_e = 100$.

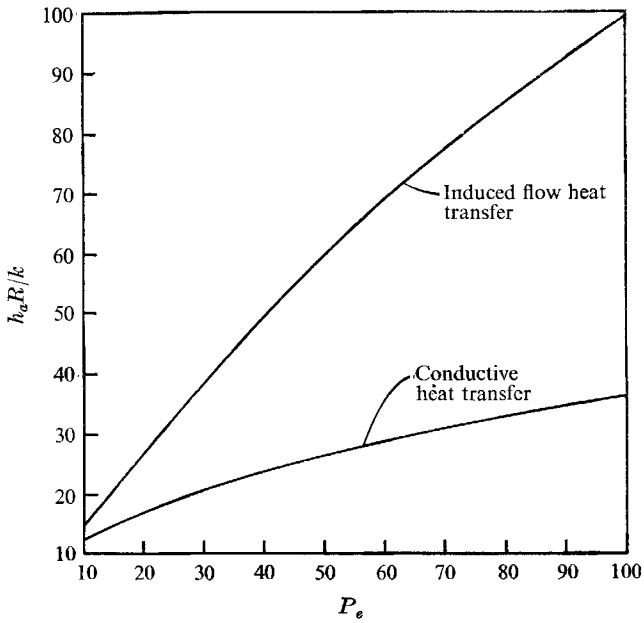

FIGURE 7. Effect of Péclet number on average Nusselt number for $t = 0{\cdot}1$.

Perhaps the best measure of the degree of enhancement due to the recirculation patterns is the comparison of the asymptotic instantaneous Nusselt numbers for induced flow and conductive heat transfer since the transient effects of temperature profile development are eliminated. This Nusselt number is necessarily independent of Péclet number for conductive heat transfer but increases from the

conduction value at $P_e = 0$ to a value for flow approximately 2·5 times as great for $P_e = 100$ as is evident from figure 8. Johns & Beckmann calculated an analogous curve from their finite-difference analysis of the circulating drop, and it is interesting to note that the degree of enhancement of heat or mass transfer from the drop is numerically quite similar to that for the cylindrical cavity.

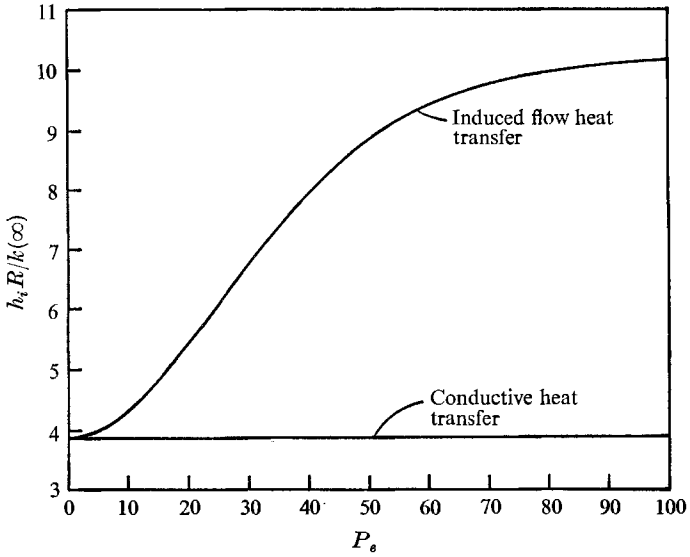

FIGURE 8. Dependence of asymptotic Nusselt number on Péclet number.

It is clear from the above results that the circulation currents induced in a liquid by the flow of tightly fitting solid particles in a tube are sufficiently strong to cause substantial heat or mass transfer enhancement if the Péclet number for the system is large enough. For the transfer of dissolved gases within blood plasma in body capillaries, the Péclet number is of the order of 1 and certainly less than 5. Hence, mass transfer enhancement will occur in this particular case only if the rate of mass transfer increases rapidly from the pure diffusion limit as the Péclet number increases. From the above heat transfer results, it can be concluded that this is not the case, and, consequently, the convective toroidal circulation contributes negligibly to the transfer of dissolved gases in the pulmonary and systemic capillaries of the body. Lew & Fung (1969) have previously proposed the same conclusion, based apparently on the reasoning that the streamline pattern, as viewed by an observer situated on the tube wall, is not significantly different from the pattern for Poiseuille flow. However, if the Peclet number is large enough (as would be the case if the diffusion coefficient of the dissolved substance in the plasma were very small), then the radial velocities would become a dominant mode of transport and would substantially increase the mass transfer rate. Indeed, as pointed out by Lighthill (1968), the transfer of complex molecules such as proteins within the systemic capillaries would be significantly enhanced by the convective motion of bolus flow because such molecules generally possess much lower diffusion coefficients than dissolved gases.

The heat transfer enhancement observed in the thermal analogue experiments of Prothero & Burton (1961) led these authors to conclude that a similar enhancement would take place in the transfer of dissolved gases in the body capillaries. The Reynolds number of the experiments of Prothero & Burton ranged from 70 to 400 and the Péclet number varied from 250 to 1200. For the low Reynolds number limit, the average Nusselt number is a function of the Péclet number, β, and t/P_e, as can readily be seen from (36). For the Prothero & Burton experiments, the average Nusselt number must, in addition, be a function of the Reynolds number. From the theoretical development and results of this investigation, it is to be expected that there should be substantial heat transfer enhancement observed in these experiments because of the high Péclet numbers utilized. The question that must be answered is whether these experiments imply increased mass transfer rates for the case of blood flow in capillaries where the Reynolds number is 0·01 or less and the Péclet number is of the order of one.

We believe that no conclusions about blood flow can be drawn from the Prothero & Burton experiments because the ranges of Péclet and Reynolds numbers are vastly different for the two cases. Prothero & Burton tried to make such a comparison by postulating that a unique relationship exists between the Nusselt number and the Graetz number (which is simply related to t/P_e) for bolus flow. It is clear from theory that this is not the case, and the effect of the Reynolds and Péclet numbers on the Nusselt number must be ascertained before experimental bolus flow heat transfer data taken at relatively high Péclet and Reynolds numbers can be used to predict bolus flow mass transfer rates at low Péclet and Reynolds numbers.

The method of analysis presented here leads to an analytical solution from which numerical results can be obtained without excessive computation. Hence, this approach may well be useful in the analysis of a variety of closed-streamline flow problems. In addition, the results presented here should provide some insight into the mechanism of heat and mass transfer for practically important bolus flow situations.

The authors are indebted to Dr R. R. Klimpel for providing a computer program for the conjugate gradient method.

REFERENCES

AMES, W. F. & DE LA CUESTA, H. 1963 *J. Math. Phys.* **42**, 301.

BURGGRAF, O. R. 1966 *J. Fluid Mech.* **24**, 113.

CARSLAW, H. S. & JAEGER, J. C. 1959 *Conduction of Heat in Solids.* Oxford University Press.

COOKE, R. G. 1953 *Linear Operators.* London: Macmillan.

DE LA CUESTA, H. & AMES, W. F. 1963 *Ind. Engng Chem. Fundamentals*, **2**, 21.

DENNIS, S. C. R. & POOTS, G. 1956 *Quart. Appl. Math.* **14**, 231.

DENNIS, S. C. R., MERCER, A. McD. & POOTS, G. 1959 *Quart. Appl. Math.* **17**, 285.

DUDA, J. L. & VRENTAS, J. S. 1970 *J. Fluid Mech.* **45**, 247.

ECKERT, E. R. G. & DRAKE, R. M. 1959 *Heat and Mass Transfer.* New York: McGraw-Hill.

GILL, A. E. 1966 *J. Fluid Mech.* **26**, 515.

GOLDFARB, D. & LAPIDUS, L. 1968 *Ind. Engng Chem. Fundamentals*, **7**, 142.

HADAMARD, J. 1911 *Comptes Rendus*, **152**, 1735.

HO, C. Y., NARDACCI, J. L. & NISSAN, A. H. 1964 *A.I.Ch.E.J.* **10**, 194.

JARRETT, E. L. & SWEENEY, T. L. 1967 *A.I.Ch.E.J.* **13**, 797.

JEFFREYS, H. & JEFFREYS, B. S. 1956 *Methods of Mathematical Physics*. Cambridge University Press.

JOHNS, L. E. & BECKMANN, R. B. 1966 *A.I.Ch.E.J.* **12**, 10.

KANTOROVICH, L. V. & KRYLOV, V. I. 1958 *Approximate Methods of Higher Analysis*. New York: Interscience.

KRONIG, R. & BRINK, J. C. 1950 *Appl. Sci. Res.* A **2**, 142.

LEW, H. S. & FUNG, Y. C. 1969 *Biorheology*, **6**, 109.

LIGHTHILL, M. J. 1968 *J. Fluid Mech.* **34**, 113.

MCADAMS, W. H. 1954 *Heat Transmission*. New York: McGraw-Hill.

OLIVER, D. R. & WRIGHT, S. J. 1964 *Brit. Chem. Engng*, **9**, 590.

OLIVER, D. R. & YOUNG HOON, A. 1968 *Trans. Inst. Chem. Engng*, **46**, T 116.

POOTS, G. 1958 *Quart. J. Mech. Appl. Math.* **11**, 257.

PROTHERO, J. & BURTON, A. C. 1961 *Biophys. J.* **1**, 565.

SINGH, S. N. 1958 *Appl. Sci. Res.* A 7, 325.

WHITTAKER, E. T. & WATSON, G. N. 1927 *Modern Analysis*. Cambridge University Press.

WILKES, J. O. & CHURCHILL, S. W. 1966 *A.I.Ch.E.J.* **12**, 161.